Aerospace Science and Technology 177 (2026) 112869

Contents lists available at ScienceDirect

Aerospace Science and Technology

journal homepage: www.elsevier.com/locate/aescte

Assessment of easily accessible and proprietary models of departure aircraft performance using open flight tracking data and a mixed analysis-synthesis approach

Lorenzo Dorbolò, Marco Pretto *, Pietro Giannattasio

Dipartimento Politecnico di Ingegneria e Architettura, University of Udine, Via delle Scienze 206, 33100, Udine, Italy

ARTICLE INFO

Editor name: Dr Yu Lv

Keywords:
Aircraft departures
Flight tracking
Aircraft performance modelling
Engine thrust
Fuel flow

ABSTRACT

Predicting the environmental impact of civil air traffic around airports requires reliable modelling of aircraft operations, especially for departures due to their high engine thrust near the ground. Assessing currently available aircraft performance models is difficult without proprietary FDR (flight data recorder) information, but the recent availability of open flight tracking data has prompted formulation of a reliable modelling tool for flight operation reconstruction using a mixed analysis-synthesis approach (MASA) previously developed by the authors. The MASA tailors prescribed ANP (aircraft noise and performance) procedures to actual flight operations, and allows assessing different performance models without using FDR data. In this work, an upgraded MASA is used to compare the departure performance predictions of BADA4, a restricted-access proprietary model, with those based for thrust on ANP, more easily accessible, and for fuel burn on the open-data ICAO Doc 9889 method. The thrust estimation is conducted using either the ANP or BADA4 sub-model, with a hybrid sub-model also tested, while extension to fuel burn is performed including Doc 9889 and BADA4 methods. After processing over 11,000 flight-tracked departures, the resulting trajectory errors and modelled thrust outputs show good reliability of ANP especially near the take-off, while BADA4 appears more accurate in higher-altitude climb phases. For fuel burn, the open-data method yields values nearly 40 % below BADA4, but the underestimation is halved when compared to literature FDR data. These results demonstrate that easily accessible thrust and fuel flow models paired with flight tracking data can provide satisfactory predictions of departure aircraft performance.

1. Introduction

The steady increase in global air traffic following the COVID-19 pandemic has renewed focus on the challenges associated with air traffic management (ATM). Between 2023 and 2024 the total air traffic measured in revenue passenger kilometres grew by 10.4% reaching a record high, and this upward trend is expected to continue, with the air travel demand projected to rise by 8 % in 2025 [1]. As these figures keep rising, ensuring safety, efficiency, and sustainability of the airspace system becomes increasingly dependent on the fidelity of air traffic simulations [2,3].

A critical component of air traffic simulations is the aircraft performance model (APM), which provides the movement of an aircraft in terms of speed, altitude, thrust, fuel burn, and aerodynamic performance. APMs form the foundations not only for flight trajectory prediction and computation, but also for assessing the impact of flight operations on airport noise and emissions of both pollutants and greenhouse gases [4], thus rendering their accuracy crucial for ATM applications. Out of the proprietary APMs one of the best known is BADA (Base of Aircraft Data) [5], developed by EUROCONTROL to simulate the aircraft performance over the entire flight envelope using proprietary information provided by the aircraft manufacturers. BADA is

Acronyms and abbreviations: ADS-B, Automatic Dependent Surveillance - Broadcast; AEED, Aircraft Engine Emissions Databank; AFE, Above Field Elevation; ANP, Aircraft Noise and Performance; APM, Aircraft Performance Model; ATM, Air Traffic Management; BADA, Base of Aircraft Data; BFFM2, Boeing Fuel Flow Method 2; CAS, Calibrated Airspeed; ECAC, European Civil Aviation Conference; EUROCONTROL, European Organization for the Safety of Air Navigation; FDR, Flight Data Recorder; ICAO, International Civil Aviation Organization; ISA, International Standard Atmosphere; MASA, Mixed Analysis-Synthesis Approach; METAR, Meteorological Aerodrome Report; MSL, Mean Sea Level; (M)TOW, (Maximum) Take-Off Weight; PDF, Probability Density Function; QAR, Quick Access Recorder; TMA, Terminal Manoeuvring Area.

* Corresponding author.
E-mail address: marco.pretto@uniud.it (M. Pretto).

https://doi.org/10.1016/j.ast.2026.112869
Received 15 December 2025; Received in revised form 19 May 2026; Accepted 9 June 2026
Available online 11 June 2026
1270-9638/

available in two main versions: the older but widely used BADA3 family, and the more recent BADA4 family. The latter comes with improved datasets for advanced estimations in the TMA (Terminal Manoeuvring Area), but at the cost of major limitations to its accessibility. Another proprietary tool is the FLIGHT-X software package [6], which enables multi-disciplinary analysis of modern civil aircraft and has been used to estimate the aircraft performance for environmental impact assessments [7,8]. In addition, commercial APMs such as Piano [9] have been employed by several researchers to estimate the performance of aircraft engines [10,11].

In order to provide reliable flight trajectory predictions, both proprietary and open APMs need to be fed with important operational variables such as aircraft weight and weather conditions, which are difficult to know for each daily flight worldwide. However, in the past 15 years the ADS-B (Automatic Dependent Surveillance-Broadcast) technology has grown very quickly, prompting ADS-B transponders to become mandatory in 2020 for non-ultra-light aircraft operated in the European airspace [12]. This has led to the open broadcasting of their positional and kinematic information, which is collected daily by thousands of ground receivers to provide large amounts of flight tracking data on dedicated websites, such as the OpenSky Network [13]. This unprecedented data availability, alongside access to public aircraft-related datasets, has fostered the development of open-source APMs, promoting transparency in the air traffic research community. A good example of this is OpenAP [14], which since 2020 has been widely adopted in studies involving aircraft performance modelling and emission estimations [15–17]. In addition, ADS-B data have been integrated into already existing frameworks, such as the aforementioned FLIGHT-X [18] and the ECAC Doc 29 method [19,20], the latter tailored to performance and emission estimations in the TMA [21–24]. Notably, the Doc 29 method works in conjunction with the ANP (Aircraft Noise and Performance) database, which, while not open, can be accessed by any parties who demonstrate a need for modelling purposes [25].

The reconstruction of civil air traffic from ADS-B data has been of particular interest for the present authors, who recently proposed an improved estimation of TMA aircraft performance using a mixed analysis-synthesis approach (MASA) based on a modified Doc 29 method [26], which was further upgraded with the inclusion of high-resolution tracking data [27]. A key feature of the authors' modelling tool, which includes the MASA as a key component, is its independence from specific performance estimation methods, which comes from the minimization of errors between tracked (*analysis*) and modelled (*synthesis*) flight trajectories. Concerning the flight performance predictions, the engine thrust estimates obtained from the ANP method were validated indirectly yet successfully using airport noise levels. This is definitely a viable solution, as confirmed also by van der Grift et al. [28], but access to clearer sources of information remains crucial.

In this work, the aircraft performance estimation is addressed directly. This was spurred by the authors' access to BADA4, proprietary APM that provides advanced sub-models and datasets to enable reconstruction of engine thrust and fuel flow over the entire flight envelope for many aircraft models. The availability of BADA4 makes it possible to compare its performance outputs with those of simpler but more easily accessible methods, when any of them is used within a reliable flight path reconstruction tool based on ADS-B data such as the authors' MASA. This comparison can provide valuable information on the strong and weak points of either model, indicating also future improvement paths. Moreover, the only tools that give direct information as to the flight performance are FDR or QAR (Quick Access Recorder) data, but their use is heavily constrained by confidentiality issues [19]. Conversely, the MASA can be deployed at an arbitrarily large scale to assess the effectiveness and reliability of any performance estimation model including BADA4 itself, acknowledged to be a powerful APM that, however, has still margins for improvement [29].

In light of these considerations, the present work tackles the aircraft performance estimation by relying on several easily accessible resources, which include the ANP method, ICAO's Doc 9889 [30], the Boeing Fuel Flow Method 2 (BFFM2) [31], and the freely available ICAO Aircraft Engine Emissions Databank (AEED) [32] . However, these thrust and fuel flow estimation methods can be easily replaced with the proprietary BADA4 ones, paving the way for a balanced comparison between the two solutions. The addition of the fuel burn estimation into the authors' modelling tool completes the TMA flight performance reconstruction, enabling prospective quantification of both noise (requiring engine thrust) and pollutant emissions (requiring fuel burn). The results, computed for a very large number of flight operations, are focused on departures of turbofan aircraft, as their high thrust near the ground is the primary cause of airport emissions [19].

This paper is structured as follows. Section 2 is dedicated to the modelling tool used to reconstruct the TMA aircraft trajectory, focusing first on its general improvements and then on the estimation of engine thrust and fuel flow during departure operations using ANP, Doc 9889, and BADA4 methods within the MASA. The results are presented in Section 3 examining the trajectory errors and engine thrust reconstructions of over 11,000 departures, to which a comparison with literature FDR data is added for further validation of the open-data-based fuel burn estimation. Conclusions and future developments are presented in Section 4.

2. Methodology

2.1. Overview of the aircraft performance modelling tool

The present aircraft performance modelling tool is largely based on the one illustrated recently by the authors [27] , and a brief overview is provided here to remind its general structure and highlight the key novelties. This tool finds its roots in the ECAC Doc 29 method [20] and the accompanying ANP database [25], which provides all the parameters necessary for estimating the TMA performance and noise of over 150 reference airframe-engine combinations, commonly referred to as ANP proxies. However, this tool is here modified to enable the performance estimation using also BADA4, either as an alternative to or in combination with the ANP database. BADA4 is similar in its structure to ANP, making its integration into the authors' tool reasonably easy. In particular, BADA4 offers sets of performance data for around 110 airframe-engine combinations, referred to as BADA4 models and having effectively the same role as the ANP proxies.

Fig. 1 briefly illustrates the overall structure of the present aircraft performance estimation tool. Firstly, daily flight tracking data and METARs (weather reports) at a specified airport are collected from the OpenSky Network [13] using the Python *traffic* library [33]. The tracking data consist of ADS-B-based positional and kinematic information with non-explicit indications of the operated aircraft, and a pre-processing stage is necessary to enrich the datasets with the information required for reliable aircraft performance modelling. The following tasks are undertaken:

- each flight operation is isolated, assigned an identifier, and categorized as departure or arrival;
- for each flight operation, the airframe and engine type are identified. Then, the resulting aircraft configuration is matched to the corresponding ANP proxy and BADA4 model;
- the weather conditions during each operation are identified using the METAR data;

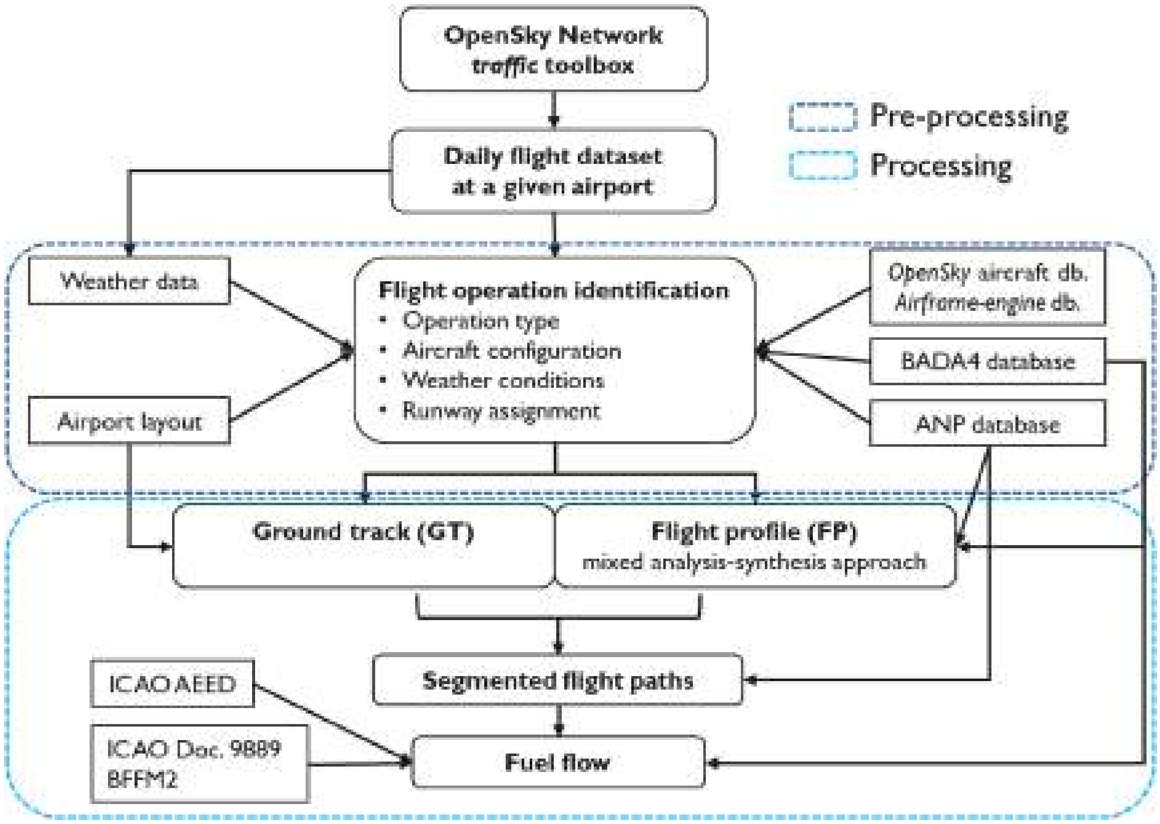

Fig. 1. Flowchart summarizing the present aircraft performance modelling tool.

- each departure / arrival is assigned a take-off / landing runway respectively, exploiting airport layout information sourced from *OurAirports* [34] and *OpenStreetMap* [35].

Each identified aircraft operation is then processed starting from the reconstruction of its ground track, after which the flight profile (aircraft performance along the ground track) is determined using the MASA, though upgraded as illustrated below, and the flight path is obtained by merging ground track and flight profile. Finally, and as a novelty compared to the previous tool [27], the fuel burn is estimated using either an open-data method that follows ICAO Doc 9889 and BFFM2 or, alternatively, BADA4. The authors' tool can also estimate airport noise levels using the Doc 29 noise engine, but this calculation falls outside the present scope.

Compared to its previous version, several new features and improvements have been included into this tool, as detailed in the remainder of this section. In particular, Section 2.2 illustrates the upgrades to the aircraft configuration identification and the MASA applied to departures. Then, Sections 2.3 Sectionsand 2.4 present, respectively, the engine thrust and fuel flow estimation models, tackling first the ANP and open-data methods and then the BADA4 procedure.

2.2. *Upgrades to the flight operation reconstruction methodology*

This section illustrates two important upgrades to the authors' modelling tool that are of general validity, i.e. independent of any flight performance sub-model. These refer to the assignment of the aircraft configuration for each operation and to the formulation of the MASA for departures.

2.2.1. *Assignment of the aircraft configuration*

In this work, the aircraft configuration is defined as the pair of airframe and engine model/variant. Notably, this piece of information is key for the computation of both noise and pollutant emissions, with possibly higher importance for the latter because the aircraft configuration influences strongly both fuel flow and pollutant emission indices [32]. Therefore, a dedicated airframe-engine database was developed relying on open data sourced not only from *Airlinerlist* [36] as in the authors' previous work [27], but also from the *rzjets* website [37], which links the aircraft registration to the engine mounted on that particular aircraft. This engine was mapped to its counterpart in the AEED, which provides reference data on thrust, fuel flow, and pollutant emissions for hundreds of actual engine models and variants [32]. Thanks to this new assignment procedure, an association could be made between aircraft registration and engine model down to the specific variant. This resulted in a more complete identification of the aircraft configuration using the registration as the key of this database, whose structure is shown in Table 1.

Following this assignment procedure, the aircraft configuration was matched to the most appropriate ANP proxy and BADA4 model using an extended version of the ANP substitution table [38], which was adapted to incorporate the mapping of BADA4 models. For the most common airliners this mapping is straightforward, whereas the occasional misidentification of some small aircraft is practically inconsequential due to their statistically negligible frequency in commercial airports.

Table 1
Structure of the airframe-engine database used for the identification of the aircraft configuration.

Registration	ICAO	Airframe	Engine	First reported on
HA-LTL	A321	A321–231	V2533-A5	22/03/2018
LV-KLE	GL5T	BD700–1A11	BR700–710A2–20	30/03/2011
EC-OBY	A21N	A321–271NX	PW1133G-JM	28/07/2023
…	…	…	…	…

Table 2
Structure of the new ANP substitution table, upgraded to include the mapping of BADA4 models.

ICAO	Airframe	Engine	ANP proxy	BADA model
A320	A320–211	CFM56–5A1	A320–211	A320–212
A320	A320–212	CFM56–5A3	A320–211	A320–212
A320	A320–214	CFM56–5B4	A320–211	A320–214
A320	A320–214	CFM56–5B4/2	A320–211	A320–214
…	…	…	…	…

The structure of this extended ANP substitution table is shown in Table 2, which shows that the same proxy can be assigned one of multiple engine variants, chosen according to the tracking data.

2.2.2. Mixed analysis-synthesis approach (MASA) for departure operations

The MASA is a modelling framework formulated by the present authors [26,27] that reconstructs the aircraft performance in the TMA by combining flight tracking data (*analysis*), typically based on ADS-B, with appropriately modified ANP flight procedures (*synthesis*). The ANP procedures consist of sets of prescribed actions during departures or arrivals, named procedural steps, that aim to represent the average flight profile of a proxy aircraft. Given the constraints of prescribed procedures, a purely synthetic profile cannot account for the massive variability of individual flights, while the straightforward use of an analytical approach is extremely challenging, due to the need for key pieces of information (e.g. flap settings, aircraft weight) that flight tracking does not provide. Instead, the MASA enables more accurate reconstruction of individual operations by introducing into the ANP procedures multiple degrees of freedom, which result in a number of optimization variables whose values are set by minimizing an objective function that measures the difference between modified synthetic ANP profile and ADS-B tracking data.

The MASA applied to departures starts from the original set of ANP procedural steps, an example of which is provided in Table 3, and the ECAC modelling framework, which enables conversion of these steps into a synthetic flight profile that provides the evolution of altitude, speed, and engine thrust over time along the ground track [20]. The ANP steps are lists of instructions that describe the actions taken by the pilot to take off and climb up to $10,000$ *ft* AFE (Above Field Elevation). As shown in Table 3, the ANP procedures are rigid, meaning that values such as target altitudes, speeds, and energy share factors (fractions of excess thrust available for acceleration) are fixed, and also flap deployment schedule and thrust cutback point (switch of engine rating from take-off to climb) cannot change. Moreover, the take-off weight (TOW) is assumed to be solely a function of a flight distance band or 'stage length', and the baseline ECAC method assumes maximum engine thrust throughout the entire departure procedure. This rigidity makes the synthetic flight profile resulting from the original set of ANP steps very different from the tracked one, but this mismatch can be significantly reduced using the MASA.

In the MASA, an appropriate number of optimization variables are identified with the aim of providing the desired degree of operational flexibility. Compared to the previous formulation [27], in this upgraded MASA up to 13 optimization variables are included. The specific details on each of them are listed in Table 4, while a general categorization can be made as follows.

- P_{type} is the profile type, which is related to the overall sequence of procedural steps and the associated flap settings. It can have up to three values, i.e. default, ICAO_A, and ICAO_B, and it is used at each optimization cycle to identify the specific set of procedural steps.
- K_T, K_C are the ratios between actual and maximum engine thrust during take-off and climb segments, respectively, and account for real-world reduced-thrust departures. As described in Section 2.3, these parameters affect the estimation of engine thrust within the ECAC-based process that synthesizes the flight profile from the ANP procedures [26].
- *TOW* is the take-off weight, which is allowed to vary continuously to account for the unknown number of passengers and the actual flight distance, which affect also the fuel load. This parameter is used at each optimization cycle in both the selection of the specific set of ANP steps and the ECAC-based flight mechanics equations that lead to the synthetic profile [20].
- Δh_j, $j = 1, 2, 3$ are the admissible height variations for the ANP target heights, to which they are summed; up to three Δh_j values are used depending on the number of climb steps below $5{,}500$ *ft*, beyond which no changes are made to ensure smooth climbing to $10,000$ *ft* (for the profile in Table 3, only two are used: Δh_1 in step 3 and Δh_2 in step 6).
- Δv_j, $j = 1, 2, 3$ are the admissible CAS (calibrated airspeed) variations for the ANP target CAS values, to which they are summed; up to three values are used: $j = 1$ covers the initial climb, $j = 2$ the CAS around flap retraction (for Table 3, steps 4 and 5), and $j = 3$ the final climb.
- $f_{e,\,j}$, $j = 1, 2, 3$ are multipliers to the energy share values, which enable redistribution of the excess thrust during each acceleration phase and work in association with Δv_j.

The first four variables had already been decided in the original approach [26], while variations of some of the ANP altitude, speed and energy share targets were added later [27]. In the present work, the freedom in target values has been extended to all departure phases and made as uniform as possible, leaving just the step sequences (which include flap sequences and thrust cutback instant) untouched within a fixed P_{type}.

The values of the optimization variables are set by minimizing an objective function, *OBF*, that is composed of two parts. The first one is RMS_{ZV}, which measures the difference in altitude and speed between ADS-B and modelled flight profiles, with custom weighting factors that emphasize the differences at lower height, much more important to reduce due to the closeness of the aircraft to the airport. The second part is a correction factor, *CF*, which acts as a penalty function aimed at

Table 3
Example of ANP departure procedural steps.

Step number	Proxy	Profile type	Stage length	Phase	Engine rating	Flap	Altitude [ft]	CAS [kt]	Energy Share [%]
1	A319–131	ICAO_B	5	Take off	*MaxTakeoff*	1+F	-	-	-
2	A319–131	ICAO_B	5	Accelerate	*MaxTakeoff*	1+F	-	169.7	68.7
3	A319–131	ICAO_B	5	Climb	*MaxTakeoff*	1+F	1,000	-	-
4	A319–131	ICAO_B	5	Accelerate	*MaxTakeoff*	1+F	-	208.8	69.2
5	A319–131	ICAO_B	5	Accelerate	*MaxTakeoff*	ZERO	-	221.2	73.0
6	A319–131	ICAO_B	5	Climb	*MaxClimb*	ZERO	3,000	-	-
7	A319–131	ICAO_B	5	Accelerate	*MaxClimb*	ZERO	-	250.0	68.8
8	A319–131	ICAO_B	5	Climb	*MaxClimb*	ZERO	5,500	-	-
9	A319–131	ICAO_B	5	Climb	*MaxClimb*	ZERO	7,500	-	-
10	A319–131	ICAO_B	5	Climb	*MaxClimb*	ZERO	10,000	-	-

Table 4
Optimization variables of the upgraded MASA applied to departures. The ranges are "up to" because occasional restrictions are necessary to prevent absurd outcomes (e.g. negative climb angles).

Variable	Symbol	Type	Values or ranges	Purpose
Procedure type	P_{type}	Discrete	Default / ICAO_A / ICAO_B	Procedural flexibility; not all procedure types are contemplated by ANP for a given proxy
Take-off thrust reduction	K_T	Continuous	$[0.75;\ 1]$	Reduced take-off thrust
Climb thrust reduction	K_C	Discrete	0.8 / 0.9 / 1	Reduced climb thrust
Take-off weight	TOW	Continuous	$[TOW_{min};\ MTOW]$	Variable weight (passengers, fuel load, distance)
First climb height	Δh_1	Continuous	Up to $[-1{,}500;\ 500]\ ft$	Flexible first group of consecutive climb steps
Second climb height	Δh_2	Continuous	Up to $[-500;\ 3000]\ ft$	Flexible second group of consecutive climb steps; not considered if already above 5500 ft
Third climb height	Δh_3	Continuous	Up to $[-500;\ 3000]\ ft$	Flexible third group of consecutive climb steps; not considered if already above 5500 ft
First CAS	Δv_1	Continuous	$[-25;\ 25]\ kt$	Flexible CAS for first group of consecutive acceleration steps
Second CAS	Δv_2	Continuous	$[-25;\ 25]\ kt$	Flexible CAS for second group of consecutive acceleration steps, if present
Third CAS	Δv_3	Continuous	$[-25;\ 25]\ kt$	Flexible CAS for third group of consecutive acceleration steps, if present
First energy share factor	$f_{e,1}$	Continuous	Up to $[0.7;\ 1.4]$	Flexible energy share factor for first group of consecutive acceleration steps
Second energy share factor	$f_{e,3}$	Continuous	Up to $[0.7;\ 1.4]$	Flexible energy share factor for second group of consecutive acceleration steps, if present
Third energy share factor	$f_{e,3}$	Continuous	Up to $[0.7;\ 1.4]$	Flexible energy share factor for third group of consecutive acceleration steps, if present

preventing unlikely operational occurrences. Among these, the most relevant are departures at low thrust and high *TOW*, which are completely prevented by other models, such as Sun et al.'s [39], while here they are just highly penalized. The expression for *OBF*, reported in Eq. (1), remains unchanged from the one defined in the previous work [27], where more details on its origin and formulation are provided.

trajectory reconstruction. Based on this reasoning, it can be expected that the analysis of the MASA outputs is a viable solution for assessing the reliability of different TMA performance estimation methods. In this work, three different thrust models are included, and the MASA is used to assess their effectiveness in Section 3.1.

Finally, the MASA for arrivals, equally based on ECAC Doc 29 [20] and described in detail by the authors [27], is not considered herein.

$$\begin{cases} OBF = RMS_{ZV} + CF = RMS_Z + 25\cdot RMS_V + CF, \\ RMS_Z = 20\cdot\sqrt{\frac{1}{N_L}\sum_{i=1}^{N_L}\left(Z_{FP,i} - Z_{ADSB,i}\right)^2} + 10\cdot\sqrt{\frac{1}{N_M}\sum_{i=1}^{N_M}\left(Z_{FP,i} - Z_{ADSB,i}\right)^2} + \sqrt{\frac{1}{N_H}\sum_{i=1}^{N_H}\left(Z_{FP,i} - Z_{ADSB,i}\right)^2}, \\ RMS_V = 20\cdot\sqrt{\frac{1}{N_L}\sum_{i=1}^{N_L}\left(V_{FP,i} - V_{ADSB,i}\right)^2} + 10\cdot\sqrt{\frac{1}{N_M}\sum_{i=1}^{N_M}\left(V_{FP,i} - V_{ADSB,i}\right)^2} + \sqrt{\frac{1}{N_H}\sum_{i=1}^{N_H}\left(V_{FP,i} - V_{ADSB,i}\right)^2}, \\ CF = RMS_{ZV}\cdot\left[\max(0, K_{MTOW} - K_T) + \left(\exp\left(\left|K_{MTOW,est} - K_{MTOW}\right|\right) - 1\right)\right]. \end{cases} \quad (1)$$

In Eq. (1) N_L, N_M, N_H, are, respectively, the number of ADS-B points at low (< 1,500 ft), medium (1,500 to 5,000 ft), and high (above 5,000) height AFE, while Z_i and V_i are the altitude and ground speed of the *i* th point given by either ADS-B or the computation (subscript *FP*). Finally, K_{MTOW} is the aircraft TOW-to-MTOW ratio, with $K_{MTOW,est}$ being the ratio estimated using the ANP lift coefficient and the lift-off speed extracted from highly resolved ADS-B data [27].

The objective function minimization is carried out using the dual annealing global optimization algorithm [40] coupled with the sequential least squares programming method [41] to conduct local searches for acceptable solutions. This solution enhances identification of the global minimum in problems where multiple local minima may exist, such as the present one [27]. During each iteration the optimization variables are systematically adjusted, gradually aligning the modified synthetic flight profile with the ADS-B data, and the process is ended as soon as the difference in *OBF* between successive iterations falls below a predefined threshold.

The MASA for departure operations has general validity, and its reliability already emerged when using earlier versions of it to improve the estimation of aircraft noise [26,27]. The MASA is capable of reconstructing the flight trajectory thanks to its reliance on flight mechanics equations, as long as an adequate thrust estimation method is used. In case the thrust model were inadequate, good predictions of flight path could be achieved, but unrealistic combinations of TOW and thrust reduction would be recorded. Conversely, forcing a good TOW-thrust combination would result in a significant error in the flight trajectory based on the ANP procedural steps, thus preventing the use of the MASA as a performance assessment tool.

This is because the engine thrust does not affect the reconstruction of the flight trajectory based on the ANP procedural steps, thus preventing the use of the MASA as a performance assessment tool.

2.3. Estimation of departure engine thrust

Consistently with the previous observations, reliable reconstruction of a departure profile requires an effective thrust estimation method, whose accuracy should be high especially near the maximum outputs typical of the take-off phase. In this work, three options are considered:

1) the more accessible ANP thrust estimation method (Section 2.3.1),
2) the BADA4 thrust estimation method, based on proprietary datasets (Section 2.3.2),
3) a hybrid method developed in accordance with the AEDT (Aviation Environmental Design Tool) guidelines [42] that combines the two methods above (Section 2.3.3).

Additionally, all methods use custom corrections to account for actual operations, as detailed below.

2.3.1. ANP thrust estimation method

The first method is based on the sub-model proposed by ECAC Doc 29 and ANP for turbofan engines [20] and it consists in the following expression:

$$\left(\frac{F_n}{\delta}\right)_{act} = K_{red}\cdot\frac{F_{0,AEED}}{F_{0,ANP}}\cdot\left(\frac{F_n}{\delta}\right)_{max} = K_{red}\cdot\frac{F_{0,AEED}}{F_{0,ANP}}\cdot\left[E + F\cdot V_C + G_A\cdot Z + G_B\cdot Z^2 + H\cdot(T - 273.15)\right] \tag{2}$$

In Eq. (2) two contributions can be isolated. The baseline contribution is $(F_n/\delta)_{max}$, which derives directly from ECAC-ANP and comes with the following definitions:

- $(F_n/\delta)_{max}$ is the maximum corrected net thrust per engine, where F_n is the net thrust and δ is the ratio between at-altitude and standard air pressure at MSL (101.3 kPa);
- E, F, G_A, G_B, and H are the proxy-dependent thrust regression coefficients, provided by ANP in separate sets for both *MaxTakeoff* and *MaxClimb* engine ratings;
- V_C is the CAS, Z is the altitude, and T is the at-altitude air temperature.

Then, $(F_n/\delta)_{max}$ is altered by the second contribution, which consists of two correction terms:

- K_{red} is the thrust reduction coefficient, which is equal to either K_T for *MaxTakeoff* engine rating or K_C for *MaxClimb* rating;
- $F_{0,AEED}/F_{0,ANP}$ is the ratio between actual and ANP rated thrust values. In particular, $F_{0,AEED}$ is the rated thrust provided by AEED [32] for the engine variant identified from the tracking data as per Section 2.2.1, while and $F_{0,ANP}$ is the rated thrust of the ANP proxy. This ratio, which ranges between 0.9 and 1.1 for basically all cases, is a novel element of this work.

The output of Eq. (2) is $(F_n/\delta)_{act}$, which is the actual (i.e. reduced) corrected net thrust per engine to be used for the departure profile reconstruction.

2.3.2. BADA4 thrust estimation method

As mentioned in the Introduction, BADA4 is an APM that provides calculation models to simulate and/or predict the entire flight envelope (take-off, climb, cruise, descent, approach) of a civil aircraft. Compared to its predecessor BADA3, one of the key targets of BADA4 was achieving higher modelling accuracy in the TMA, which led to a close collaboration with the main aircraft manufacturers to provide several highly detailed performance estimation sub-models [43]. However, this proprietary nature led to strong restrictions for users, which include strict access requirements, no sharing of datasets, and a dissemination of results that prevents explicit reference to specific aircraft types. For the purposes of the present work, only the engine thrust and fuel flow estimation methods provided by BADA4 for turbofan aircraft were considered.

The BADA4-based expression for computing non-idle actual corrected net thrust per engine $(F_n/\delta)_{act}$ is given by Eq. (3):

$$\left(\frac{F_n}{\delta}\right)_{act} = \frac{F_{0,AEED}}{F_{0,BADA}}\cdot K_{red}\cdot\frac{g\cdot m_{ref}}{N_{eng}}\cdot C_T(M,\delta,\theta). \tag{3}$$

Similarly to Eq. (2), this expression as well includes correction coefficients $F_{0,AEED}/F_{0,BADA}$ and K_{red}, which retain the same purposes as above. The only difference is the use of $F_{0,BADA}$, which is the rated thrust of the unique AEED engine variant associated with the BADA4 aircraft model. The rest of Eq. (3) constitutes the unaltered BADA4 thrust estimation sub-model, where:

- g is the gravitational acceleration, m_{ref} is the reference mass of the BADA4 aircraft model, and N_{eng} is its number of engines;
- C_T is the thrust coefficient, which depends on Mach number M, pressure ratio δ, and temperature ratio θ (ratio between at-altitude and standard MSL air temperature, 288.15 K).

If the MSL temperature is below 298.15 K (flat-rated area), coefficient C_T does not depend on θ, and it becomes a function of only M and δ through throttle parameter δ_T as follows:

$$C_T = \sum_{j=0}^{5}\left[\sum_{i=0}^{5} a_{6j+i+1}M^i\right]\delta_T^j, \quad with\ \delta_T = \sum_{j=0}^{5}\left[\sum_{i=0}^{5} b_{6j+i+1}M^i\right]\delta^j\ . \tag{4}$$

For higher temperatures δ_T is more complex and depends also on θ, while for idle ratings C_T has a different expression altogether. However, since these conditions are not considered in this work, the reader is referred to the BADA4 manual for the relevant sub-models [43].

For a given engine rating C_T depends on 72 (i.e. 36 for both a_k and b_k) regression coefficients, which is a much larger amount than ANP that aims to capture more finely the variation of engine thrust with speed and altitude. Moreover, for departures two separate ratings named *MaxTakeoff* and *MaxClimb* are generally considered and assigned different coefficients, similarly to ANP. However, unlike ANP, not all BADA4 models have the *MaxTakeoff* rating, in which case the *MaxClimb* rating is extended to the take-off phase. Finally, it is noted that the regression coefficients are provided by BADA4 in accordance with the aircraft manufacturers, and as such their values cannot be disclosed.

2.3.3. ANP-BADA4 hybrid thrust estimation method

Although the BADA4 formulation is more refined than ANP's, the possible absence of *MaxTakeoff* ratings may give rise to inconsistencies. Aware of this, AEDT proposes in its manual [42] a thrust estimation method that pairs the benefits of BADA4 with the higher generality of the ANP sub-model when using ANP procedural steps. This method, denoted as 'hybrid', is implemented as follows:

- the ANP steps that require *MaxTakeoff* engine rating are always modelled using the ANP thrust estimation method, even if the BADA4 *MaxTakeoff* rating is available;
- the ANP steps that require *MaxClimb* engine rating are always modelled using the BADA4 thrust estimation method.

This solution should enable consistent estimation of the peak thrust output near the lift-off point, while preserving BADA4's finer estimation for the longer-lasting climb portion.

2.4. Estimation of departure fuel burn

Application of the upgraded MASA of Section 2.2 using any of the thrust estimation methods of Section 2.3 enables reconstruction of the aircraft performance during a departure. This yields the evolution of speed, altitude, and especially engine thrust along the ground track, which can be used as a key input for estimating the fuel flow. In this work, two estimation methods are considered:

1) an open-data-based method that relies on the AEED [32] and the ICAO Doc 9889 'twin quadratic interpolation' approach (Section 2.4.1) [30];
2) a proprietary method based on BADA4's fuel flow estimation sub-model (Section 2.4.2).

Both methods assume Jet A-1 as fuel and yield one-engine fuel flow $\dot{m}_f(t)$, which can be integrated over the departure operation to obtain total departure fuel burn M_f according to Eq. (5) below:

$$M_f = N_{eng}\int_{start}^{end}\dot{m}_f dt. \tag{5}$$

Finally, in the MASA it is assumed that the aircraft mass lost due to fuel burn, i.e. M_f, does not affect the flight profile reconstruction. This is because M_f is less than 0.5 % of the MTOW (see Section 3.2), which can be considered negligible for the present purposes.

2.4.1. ICAO Doc 9889 fuel flow estimation method

The ICAO Doc 9889 fuel flow estimation method relies on the publicly available AEED [32]. This database provides, for hundreds of turbofan engines, the fuel flows in the four standard modes of the LTO (Landing-and-Take-Off) cycle, each of which is associated with a fixed percentage of the rated thrust of a given engine, denoted as power setting. These modes are take-off, climb-out, approach, and idle, and the respective power settings are 100 %, 85 %, 30 % and 7 %. The AEED fuel flow values are valid for ISA (International Standard Atmosphere) sea-level conditions. The Doc 9889 method enables calculation of the fuel flow values at any non-AEED thrust level, although the method is recommended only for levels above 60 % [30].

For a given departure performed by an aircraft whose AEED engine was identified as reported in Section 2.2.1, the Doc 9889 method works as follows. Using the instantaneous engine thrust level, $F_{\%}$, the calculation of one-engine reference fuel flow $\dot{m}_{ref}$ is carried out according to Eq. (6):

$$\dot{m}_{ref} = \left(A \cdot F_{\%}^2 + B \cdot F_{\%} + C\right) \cdot \dot{m}_{ref,100\%}, \tag{6}$$

where $\dot{m}_{ref,100\%}$ is the reference fuel flow value corresponding to 100 % thrust, and coefficients A, B and C are obtained through the quadratic fitting of three pairs of fuel flow and thrust level values reported by AEED for the identified engine. These coefficients are determined by solving the three-equation system in (7):

$$\begin{cases} Y_1 = A \cdot F_{\%,1}^2 + B \cdot F_{\%,1} + C, \\ Y_2 = A \cdot F_{\%,2}^2 + B \cdot F_{\%,2} + C, \\ Y_3 = A \cdot F_{\%,3}^2 + B \cdot F_{\%,3} + C, \end{cases} \tag{7}$$

where Y_i is the ratio of the i th AEED fuel flow value to $\dot{m}_{ref,100\%}$, and $F_{\%,i}$ is the corresponding thrust level. For $F_{\%} \geq 85$ %, the power settings are 100 %, 85 % and 30 % with the respective fuel flows, while for $F_{\%} <$ 85 % the interpolation uses the 85 %, 30 % and 7 % settings, resulting in the aptly named 'twin quadratic interpolation'. Then, Eq. (8) from BFFM2 [31] is used to account for non-reference (i.e. non-ISA-sea-level) atmospheric conditions:

$$\dot{m}_f = \dot{m}_{ref} \cdot \frac{B_m \cdot \delta}{\theta^{3.8} \cdot e^{0.2 \cdot M^2}}, \tag{8}$$

where $\dot{m}_f$ is the actual non-reference fuel flow, and B_m is a mode-specific adjustment factor that increases the fuel flow to account for the activation of the environmental control system. This increment is minimal, with $B_m = 1.01$ in take-off mode and $B_m = 1.013$ in climb mode.

In the present computation, the key input other than the AEED is thrust level $F_{\%}$, the computation of which is not addressed by Doc 9889. Following other fuel flow estimation methods [44], it was decided to estimate this level as $F_{\%} = (F_n/\delta)_{act}/F_{0,AEED}$, which is the ratio between at-altitude thrust $F_{n,act}$ scaled to its ISA sea-level equivalent via pressure ratio δ and actual rated thrust $F_{0,AEED}$.

2.4.2. BADA4 fuel flow estimation method

As anticipated in Section 2.3.2, BADA4 provides a fuel flow estimation sub-model based on proprietary datasets. The portion of this sub-model valid for non-idle engine ratings is presented in Eq. (9), and it enables computation of one-engine non-reference fuel flow $\dot{m}_f$ as

$$\dot{m}_f = \frac{\dot{m}_{ref,100\%,AEED}}{\dot{m}_{ref,100\%,BADA}} \cdot \frac{\delta \cdot \theta^{0.5} \cdot a_0}{LHV} \cdot \frac{g \cdot m_{ref}}{N_{eng}} \cdot C_F(M, \delta, \theta),$$
$$\text{with } C_F = \sum_{j=0}^{4} \left[\sum_{i=0}^{4} f_{5j+i+1} C_T^i \right] M^j, \tag{9}$$

where LHV is the lower heating value of the fuel, a_0 is the ISA sea-level speed of sound, and C_F is a dimensionless fuel flow coefficient that depends on Mach number M and thrust coefficient C_T through 25 regression coefficients f_k per engine rating. To account for the actual engine, the fuel flow is corrected using $\dot{m}_{ref,100\%,AEED}/\dot{m}_{ref,100\%,BADA}$, which is the AEED-to-BADA ratio of reference flows at 100 % thrust, with $\dot{m}_{ref,100\%,BADA}$ being the AEED flow for the specific engine associated with the BADA4 aircraft model. Moreover, while in the original BADA4 method C_T is computed simply using Eq. (4), the thrust corrections introduced above required generalizing its calculation. This was done using $(F_n/\delta)_{act}$, which was plugged into Eq. (10) to calculate C_T as

$$C_T = \left(\frac{F_n}{\delta}\right)_{act} \cdot \frac{N_{eng}}{g \cdot m_{ref}}. \tag{10}$$

It is straightforward to notice that Eq. (10) coincides with Eq. (3) when BADA4 is used without corrections, and C_T is estimated using Eq. (4) as expected. However, this generalization enables use of any thrust estimation methods, including those presented in Section 2.3.

3. Results

The validation of the aircraft performance estimation methods proposed in this work is split into two sections. Firstly, Section 3.1 is dedicated to the flight profile calculation, which is conducted by applying the MASA with the thrust estimation methods listed in Section 2.3 to the flight tracking data collected for several thousand departures from multiple airports. The outcomes are evaluated focusing on thrust levels and two kinematic error parameters purposely defined to quantify the consistency of the reconstruction. Following this assessment, Section 3.2 presents an analysis of the fuel burn estimates obtained using both the Doc 9889 and the BADA4-based fuel flow estimation methods, which is completed by a fuel burn validation using literature FDR data on two aircraft models [44].

Finally, in accordance with the restrictions mentioned in Section 2.3.2, all assessments that involve BADA4 must be conducted so that the aircraft model cannot be identified. Therefore, in this work the analysis is carried out mainly on a statistical basis, whereas the FDR-based fuel burn validation includes only the Doc 9889 method since the aircraft models are known.

3.1. Flight profile estimation for departure operations

The flight profile estimation for departure operations is based on the MASA, which is applied three times, one for each of the thrust estimation methods in Section 2.3, for every departure operation. This leads to three types of reconstructed flight profile:

1) the *ANP profile*, computed using the ANP-based thrust estimation method (Section 2.3.1);
2) the *BADA4 profile*, obtained using the BADA4-based method (Section 2.3.2);
3) the *hybrid profile*, which uses the hybrid ANP-BADA4 method (Section 2.3.3).

These profiles can be compared to the ADS-B altitudes and speeds that form the *ADS-B profile*, which is considered the 'ground truth' for assessing the estimation accuracy. This assessment is carried out by defining two error parameters, computed every 1,000 ft along the ground track as follows:

$$\begin{cases} \Delta_{Z,i} = Z_{fp,i} - Z_{ADSB,i}, \\ \Delta_{V,i} = V_{fp,i} - V_{ADSB,i}. \end{cases} \tag{11}$$

In Eq. (11), $Z_{fp,i}$ and $Z_{ADSB,i}$ are the reconstructed and ADS-B altitudes, respectively, while $V_{fp,i}$ and $V_{ADSB,i}$ denote the reconstructed and ADS-B ground speed values. At the i th ground track point, their differences result in altitude error $\Delta_{Z,i}$ and ground speed error $\Delta_{V,i}$.

An example of the effectiveness of MASA is shown in Fig. 2. The plots illustrate, for a departure of an unspecified aircraft model, the large improvement achieved as the calculation goes from relying on the baseline profile indicated by ANP (i.e. P_{type} = 'default' with no optimization) to using the MASA with the ANP thrust estimation method. The improvement in terms of ratio between MASA and default RMS_{ZV} as defined in Eq. (1) is about 91 %, which is on par with the best outcomes in the authors' previous work [27] and translates into a negligible altitude error Δ_Z and a small speed overestimation $\Delta_V \in [5;\ 10]$ *kt* after the lift-off. Such a large improvement implies more realistic aircraft weight and thrust estimates, the analysis of which is carried out in the following subsections.

The large-scale calculation was conducted using the tracking data of about 11,750 departures that took place in spring 2024 in six European airports (Frankfurt, Madrid, Paris-Orly, Schiphol, Toulouse, and Zurich). The operations were chosen so that a statistically significant number of departures were available for all the common models built by the major aircraft manufacturers. The MASA was then applied to each departure, followed by a preliminary analysis of the results. From this analysis, it turned out that the BADA4 thrust estimation method yielded very different outcomes based on its behaviour near the lift-off point. Hence, the departures were split into two groups:

1) Group 1, which hosts the operations performed by BADA4 models that include either *i)* specific *MaxClimb* and *MaxTakeoff* engine rating datasets, or *ii)* only *MaxClimb* rating datasets that manage to yield values near the rated thrust of the engine, $F_{0,BADA}$, also at lift-off (i.e. $\delta \cong 1$, $M \cong 0$);
2) Group 2, which hosts those of BADA4 models where the *MaxClimb* rating datasets never yield thrust values close to expected rated thrust $F_{0,BADA}$, even at lift-off ($\delta \cong 1$, $M \cong 0$).

It is noted that the BADA4 lift-off thrust is not expected to match perfectly the rated thrust, because in the BADA4 calculation, like in the ANP one, the engines are mounted on the aircraft and $M \cong 0$ is technically outside the model applicability range. Instead, the present distinction is made with regard to the substantial thrust increase as the speed drops to zero, which Group 1 aircraft cover but Group 2 do not. Although these differences are being phased out over time with newer BADA4 versions, for the v4.2 used here (and most recent as of late 2025) this split remains fully relevant. The BADA4 models belonging to each group cannot be disclosed, suffice it to say that very common models appear in both groups and that Group 1 is marginally larger than Group 2.

3.1.1. Departure profile estimation for Group 1 aircraft models

The analysis starts from the Group 1 aircraft, and it is conducted by examining the outputs of the mixed approach. As noted in the previous work [27], the key outputs are the estimates of weight (TOW) and take-off engine thrust, which are shown in Fig. 3 as distributions of $K_{MTOW} = TOW/MTOW$ and take-off thrust reduction coefficient K_T for the ANP, BADA4, and hybrid estimation methods. These distributions provide valuable insight into the response of these methods, because normally thrust reduction is applied as much as possible to preserve the engine lifespan but only when the TOW is low enough to allow for a safe lift-off, which leads to K_T and K_{MTOW} being roughly equal [27]. Indeed, Fig. 3 shows that the K_T-K_{MTOW} pairs are consistent with this expectation for all thrust models, either accumulating around the $K_T = K_{MTOW}$ line (dashed straight black line) or favouring a reasonable $K_T < K_{MTOW}$ condition. The K_{MTOW} PDFs (Probability Density Functions) of the three methods are also similar, whereas in the K_T distribution of BADA4 a stronger skew towards higher values can be noted. This suggests that BADA4 yields lower thrust values compared to ANP around the lift-off point, which the MASA compensates by slightly raising K_T during the optimization.

These considerations are further supported by Fig. 4, which compares the altitude errors, Δ_Z, the speed errors, Δ_V, and the corrected net thrust per engine normalized by the rated thrust, $(F_n/\delta)_{act}/F_0$, for the ANP, BADA4 and hybrid flight profiles. The three parameters are plotted as a function of the ADS-B height AFE, and each subplot hosts three solid lines, which represent the mean value of the parameter, enclosed into narrow shaded bands, which denote the 95 % confidence intervals. The plots are split into the three height intervals indicated in Section 2.2.2, namely low (up to 1, 500 *ft*), medium (1,500 to 5, 000 *ft*) and high (5,000 to 10, 000 *ft*), with bounds demarcated by dashed segments.

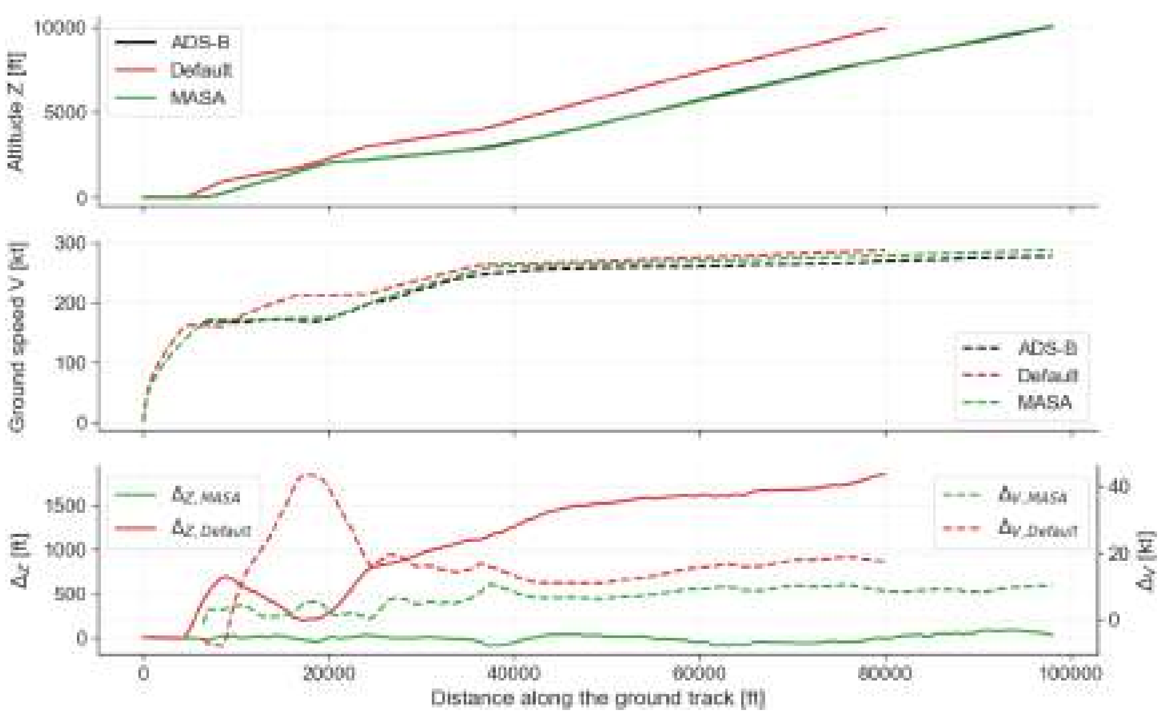

Fig. 2. A departure profile reconstruction using the default ANP solution and the MASA compared to the ADS-B profile, followed by plots of errors against ADS-B altitude, Δ_Z, and speed, Δ_V, for both profiles.

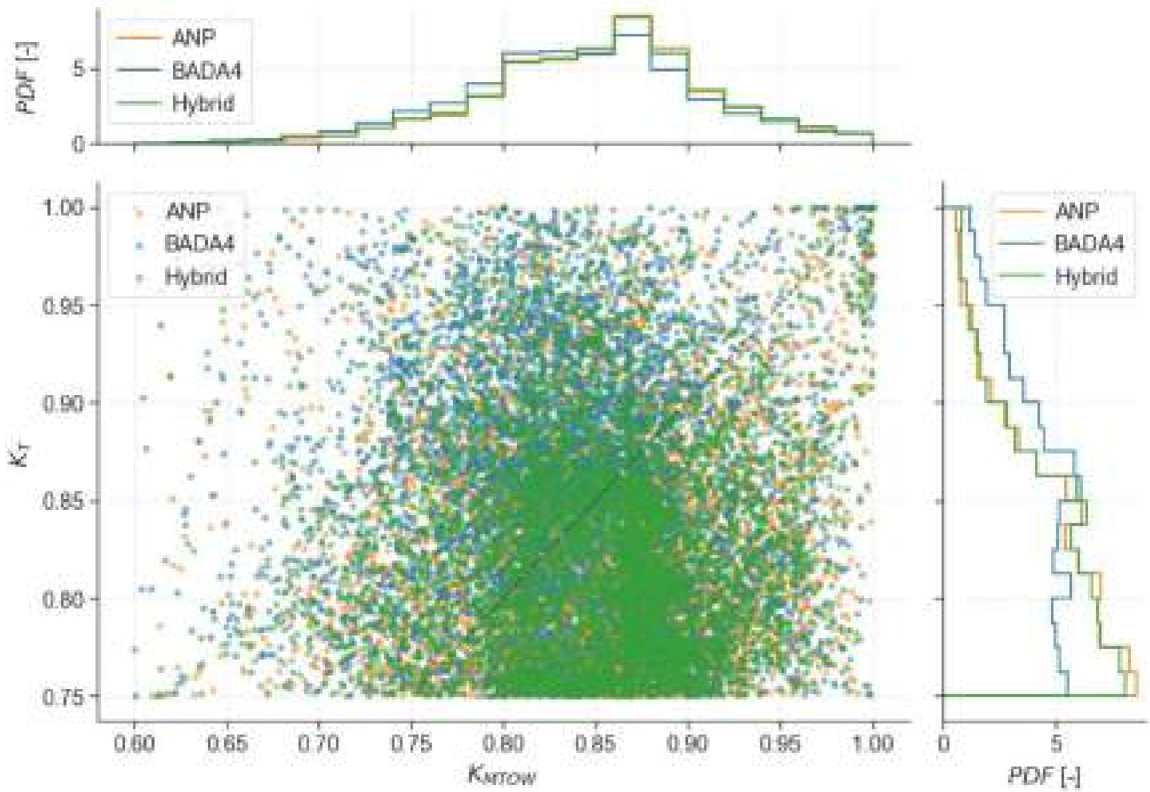

Fig. 3. Distributions of K_T and K_{MTOW} values for ANP, BADA4 and hybrid flight profiles of Group 1 aircraft, expressed as scatter plots and accompanied by separate PDFs for K_T and K_{MTOW}.

Starting from the low-height interval, the three reconstructions appear rather similar, although, as suspected from Fig. 3, the ANP and hybrid methods have indeed a marginally higher thrust than BADA4, which leads to a minor speed overestimation. In the mid-height range the results are also good, with all three methods yielding quite small and very similar errors, as well as basically equal thrust outputs. Instead, clearer differences emerge near the top of the climb, where the ANP profiles exhibit increasingly larger errors compared to their BADA4 and hybrid counterparts, which remain close to each other as they share the same thrust estimation method at similar K_{MTOW}. This declining accuracy stems from the lower ANP thrust, which, being K_{MTOW} essentially equal, causes the aircraft to climb less steeply and more slowly, resulting in a

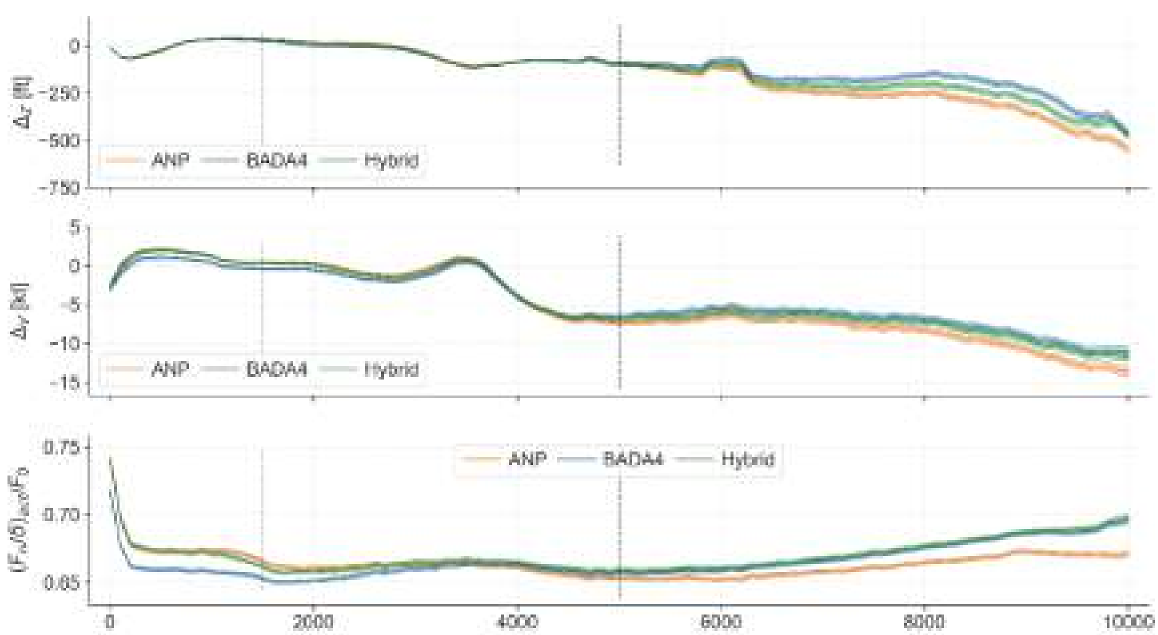

Fig. 4. Altitude errors Δ_Z and speed errors Δ_V between ANP, BADA4, and hybrid flight profiles and ADS-B trajectories for Group 1 aircraft, followed by plots of normalized corrected net thrust per engine $(F_n/\delta)_{act}/F_0$.

higher underestimation of both altitude and speed.

After this analysis, it can be argued that the ANP-based performance reconstruction within the MASA for Group 1 aircraft models is reasonably good, yielding results that agree quite well with the proprietary BADA4 solution. Minor discrepancies appear after the take-off and in the final climb, but they can be explained by the rougher thrust estimation of Eq. (2) against Eqs. (3) and (4).

3.1.2. Departure profile estimation for Group 2 aircraft models

The same analysis is now carried out for the departures of Group 2 aircraft models. Firstly, the distributions of K_{MTOW} and K_T for the ANP, BADA4, and hybrid profiles are shown in Fig. 5. It can be immediately observed that ANP and hybrid distributions are not only similar to each other, as expected since they have identical take-off thrust estimation methods, but also that they are close to those in Fig. 3, although both K_T and especially K_{MTOW} trend towards higher values. On the contrary, the BADA4-based distributions of both K_{MTOW} and K_T are markedly different from their Fig. 3 counterparts, with a much lower average K_{MTOW} and a marked tendency towards $K_T \cong 1$. This is arguably unrealistic from an operational standpoint, as in real-world departures low weights are normally associated with noticeably reduced thrust outputs due to the engines being chosen so that their maximum thrust enables the aircraft to take off at MTOW [27]. This suggests that the BADA4 thrust estimation for Group 2 aircraft models might be unsuited for the take-off stage.

This observation is confirmed by Fig. 6, which hosts the same plots of altitude error, speed error, and normalized corrected net thrust per engine as a function of ADS-B height described in Fig. 4. Indeed, near the ground all BADA4 profiles exhibit consistently larger errors compared to the other two, and this is particularly true for speed error Δ_V, which peaks at −15 kt in the initial climb (around 500 ft AFE) compared to the −6 kt of ANP and hybrid profiles. The root cause of this discrepancy is the fact that the BADA4 thrust is about 15 % lower than ANP, with a maximum of 20 % during the take-off roll (i.e. at 0 ft AFE). Since take-off roll length s_{TO} in ECAC is such that $s_{TO} \propto TOW^2/F_n$, this low thrust coupled with the mixed approach attempting to preserve the s_{TO} reported by ADS-B leads the TOW, and hence K_{MTOW}, to decrease. Then, since in the ECAC initial climb $TOW \propto V^2$, the aircraft speed drops quickly, resulting in the observed speed underestimation. These elements suggest that the ANP thrust estimation method may be capable of a better take-off reconstruction for the aircraft models in Group 2.

The thrust differences seem to extend to the remainder of the reconstruction. In the mid-height region, the BADA4 thrust remains much lower than the ANP one, causing again a speed underestimation until about $3,500\ ft$, where finally the ANP and hybrid thrust values approach the BADA4 ones due to the thrust cutback to climb rating. This compounds with the unlikely low BADA4 K_{MTOW}, leading to an easier aircraft acceleration that ultimately results in the BADA4 Δ_V becoming the closest to zero by $5,000\ ft$ AFE. Beyond this height, the error profiles start to diverge measurably from each other. Here the BADA4 profiles appear to be the best-performing ones, but this is only a result of the K_{MTOW} effect noted earlier, which allows the aircraft to achieve near-zero Δ_Z and small $\Delta_V \cong -4\ kt$ despite the low thrust. On the other hand, the ANP profiles have highest thrust but also high K_{MTOW}, which forces a lower climb angle and results in higher Δ_Z alongside a modest speed underestimation ($\Delta_V \cong -8\ kt$). Finally, the worst reconstruction is given by the hybrid method, which combines the high yet reasonable ANP-based K_{MTOW} estimate with the lower climb thrust of BADA4, causing the aircraft to climb both too gently (largest absolute Δ_Z) and too slowly (largest absolute $\Delta_V \cong -12\ kt$).

From the results obtained for both Group 1 and Group 2, two key conclusions can be drawn. Firstly, the MASA is confirmed to be a good strategy for reconstructing the flight profile, thanks to its minimization of kinematic errors regardless of the thrust prediction method applied. Secondly, the ANP method appears capable of providing a reliable output across all aircraft types. The proprietary BADA4 method behaves

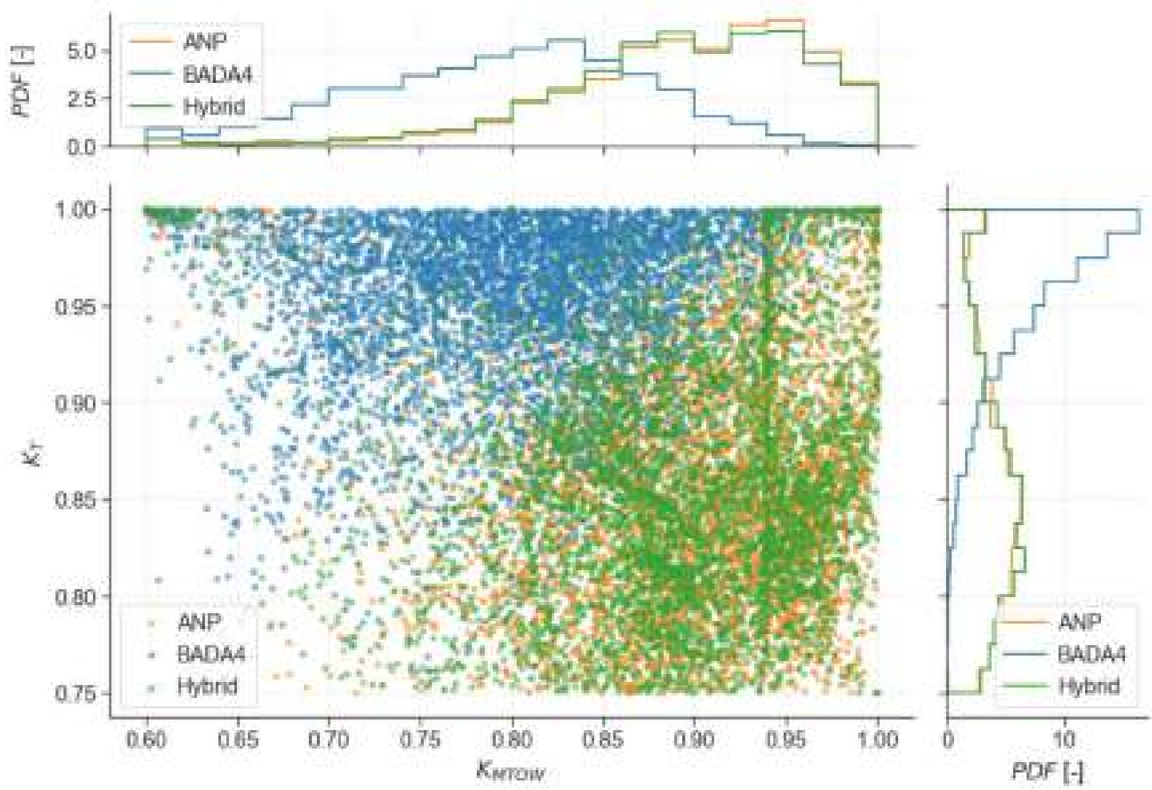

Fig. 5. Distributions of K_T and K_{MTOW} values for ANP, BADA4 and hybrid flight profiles of Group 2 aircraft, expressed as scatter plots and accompanied by separate PDFs for K_T and K_{MTOW}.

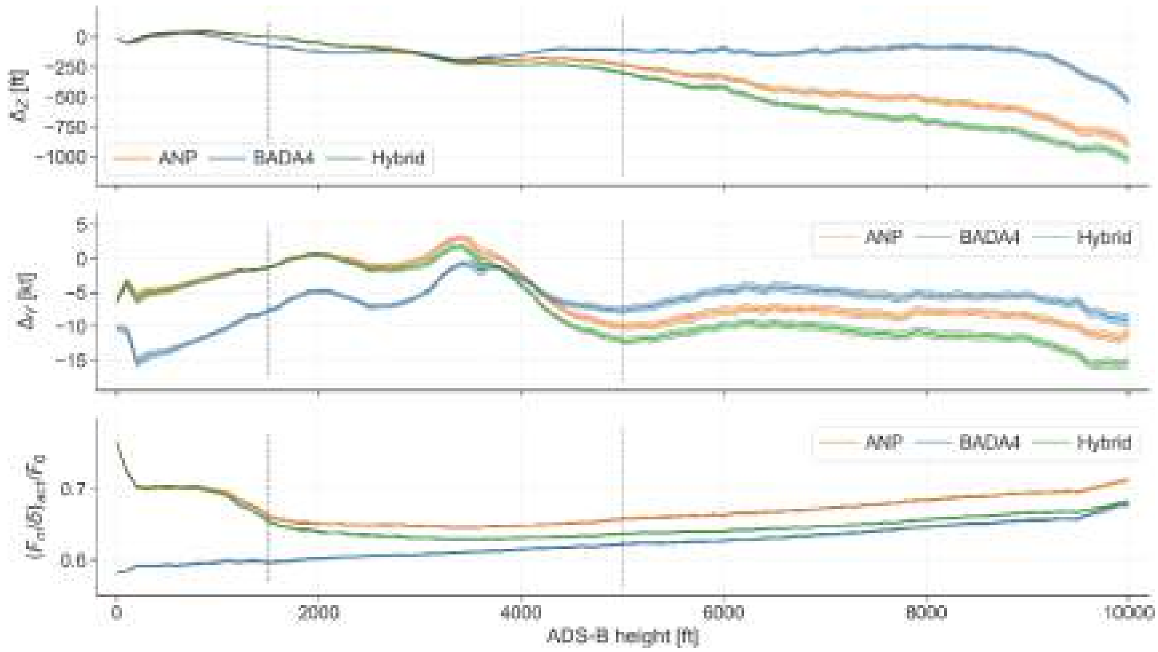

Fig. 6. Altitude errors Δ_Z and speed errors Δ_V between ANP, BADA4, and hybrid flight profiles and ADS-B trajectories for Group 2 aircraft, followed by plots of normalized corrected net thrust per engine $(F_n/\delta)_{act}/F_0$.

better at high altitudes, but the higher uniformity of ANP in the estimated peak thrust near the take-off is a noticeable benefit, which compounds with the advantage of being more easily available. Finally, combining BADA4 with ANP in the hybrid method leads to minor advantages for the favourable Group 1 case, but for Group 2 major reconstruction errors are observed.

3.2. Estimation of fuel burn during departure operations

The analysis now moves to the fuel burn estimation, which was conducted using the ANP thrust estimation method in light of its consistency across aircraft models. To carry out this analysis, in the first step the ANP profiles of all departure operations in Section 3.1 were taken

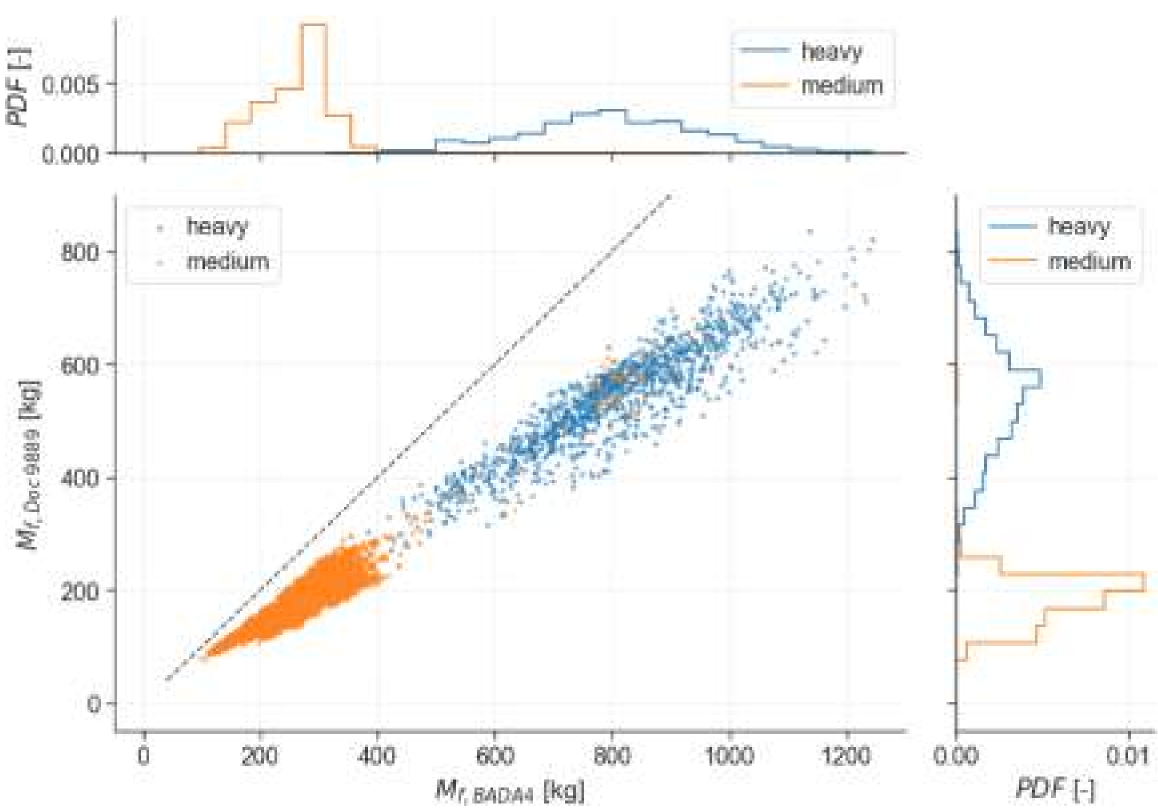

Fig. 7. Comparison of fuel burn estimates from Doc 9889 and BADA4 methods for the departures of Section 3.1. The ANP thrust method is used, and the aircraft are split into 'medium' and 'heavy' categories.

and, for each of them, the one-engine fuel flow was calculated using both Doc 9889 and BADA4 methods. Both fuel flows were then integrated using Eq. (5) to obtain two fuel burn estimates M_f for each departure. The results are reported in Fig. 7, which shows the fuel burn predictions for two different sets of aircraft, categorized into small- and mid-sized aircraft, denoted as 'medium', and heavy aircraft using a MTOW cut-off of $300,000$ *lb* (i.e. $136,077$ *kg*). Each point represents an individual departure, with its *x*-coordinate given by the BADA4 M_f and its *y*-coordinate by the Doc 9889 M_f, while the dashed black line indicates the line of equality, along which the results of two methods yielding identical outcomes would accumulate. All data points lie below this line, meaning that the Doc 9889 method consistently predicts lower fuel burn than BADA4. For 'medium' aircraft the BADA4 M_f is on average 39 % higher, while for the 'heavy' ones the difference is even wider, with BADA4 estimates averagely 45 % higher than those based on Doc 9889. Nevertheless, in all cases the M_f values are of order $10^2 - 10^3$ *kg*, which is consistent with the assumption of $M_f/MTOW < 0.5$ % and corroborates the simplification of neglecting M_f in the profile estimation.

Although clear systematic differences exist between the estimation methods based on Doc 9889 and BADA4, this analysis does not yet prove the accuracy of either method. This can be done only using real-world data, typically derived from FDRs or QARs, but this information is usually deemed confidential and cannot be shared or shown. However, one of the very few cases with publicly available fuel burn amounts from FDRs is Senzig et al.'s work [44], where comparisons are made between their fuel burn estimation method and the FDR reports for a few hundred departures of Boeing 757–200 (a 'medium' aircraft) up to $3,000$ *ft* AFE and a similar number of Boeing 777–300ER (a 'heavy' aircraft) departures up to $10,000$ *ft* AFE. The FDR fuel burn values were extracted by digitizing Figs. 1 and 4 of their paper, which enabled setting up a comparison against the open-data-based Doc 9889 method, whereas the BADA4 estimates cannot be shown for licence restrictions.

Since the original FDR flight profiles are not available, in this work a large set of departure profiles was generated synthetically for both aircraft models by varying all optimization variables listed in Table 4 using randomized inputs. This led to the synthesis of a broad range of vertical flight profiles, from which fuel flow and total fuel burn could be computed. For this synthesis, all Boeing 757–200 were assumed to be equipped with RB211–535E4 engines, while all Boeing 777–300ER with the GE90–115B engines. ISA conditions were assumed for all synthesized departures.

Fig. 8 shows the comparison between the statistical dispersions of fuel burn from Doc 9889 (solid lines) and FDR data (dashed lines) for the two aircraft. The significant differences in fuel burn between the two are due to a combination of different cut-off heights, $3,000$ *ft* against $10,000$ *ft* AFE, and different *MTOW*, around $115,000$ *kg* against $350,000$ *kg*. Firstly, for the smaller 757–200 there is a moderate shift between estimated and FDR-based fuel burn dispersions at $M_f \cong 300$ *kg*, with the Doc 9889 model underestimating the fuel burn by 14.3 % on average. The calculation is a bit worse for the larger 777–300ER, where the shift between the two distributions is larger and the average fuel burn underestimation rises to 24.4 %.

These fuel burn predictions cannot be considered comprehensive, but they point to a few trends. In particular, the open-data Doc 9889 method seems biased towards a systematic underestimation of fuel burn compared to BADA4, but the underestimation appears lower when compared to FDR data especially in the first part of the departure, i.e. up to $3,000$ *ft* AFE. Although these discrepancies are bound to stem from many reasons, an important one is likely to be the $F_{\%} = F_n/\delta$ assumption for the Doc 9889 thrust level, which disregards factors such as air temperature and aircraft speed that instead BADA4 considers. Focus on these elements will be placed in future developments.

4. Conclusions

The many sustainability challenges posed by the worldwide air traffic increase require accurate modelling of aircraft operations, which is typically conducted with APMs. However, established APMs see access restrictions due to their reliance on proprietary datasets, while open-source APMs based on publicly available data continue to seek validation. In this context, the present authors recently proposed a tool for modelling aircraft trajectories in the TMA through a mixed analysis-synthesis approach (MASA) that minimized the error between synthetic flight profiles and the aircraft trajectories reported by flight tracking. The MASA can accept any performance estimation method, and for departure operations it is able to correlate the trajectory reconstruction quality with the outputs of the thrust estimation process. These features

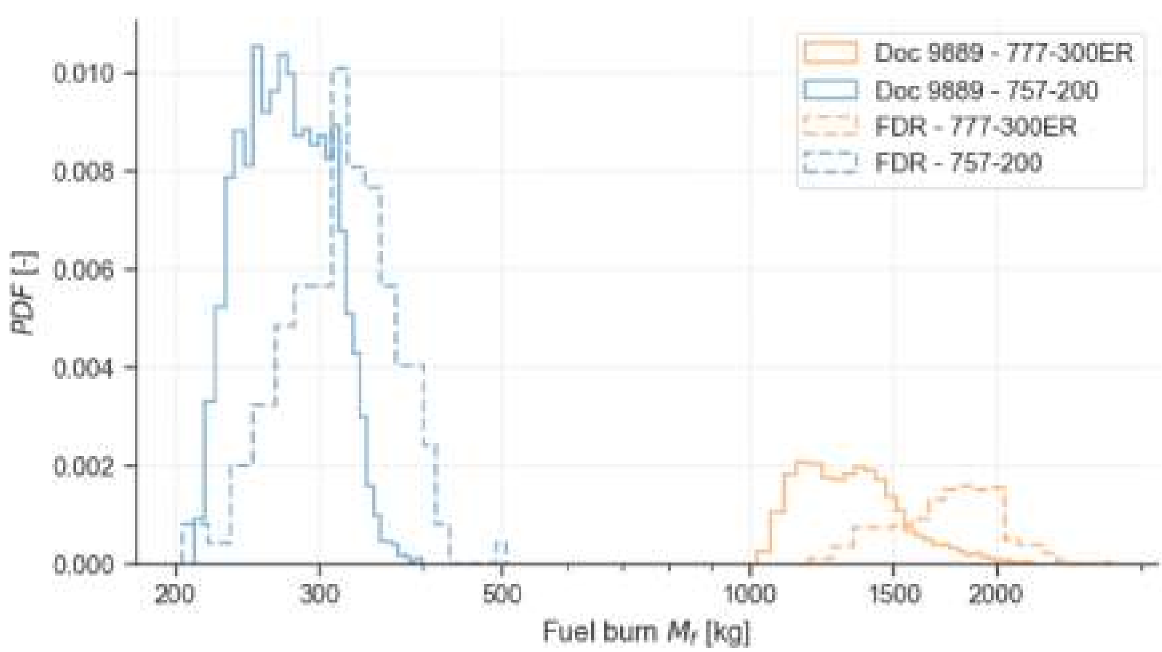

Fig. 8. PDFs of fuel burn for Boeing 777–300ER and Boeing 757–200 aircraft models. Comparison between FDR data from literature [44] and present estimates computed using the ICAO Doc 9889 method.

enable the use of MASA as a tool for comparing easily accessible modelling solutions with proprietary APMs, which is done in this work exploiting the access to BADA4. After outlining the authors' tool, the paper presents some general upgrades to flight identification from open datasets and to the MASA for departures. Emphasis is then placed on the aircraft performance, calculated through alternative use of three thrust estimation methods, i.e. the ANP method, the BADA4 method, and a hybrid between the two, and two fuel burn estimation methods, i.e. the open-data ICAO Doc 9889 method and the BADA4 one. The results are assessed on a statistical basis, analyzing trajectory reconstruction errors and performance outputs for over 11,000 departures, to which a comparison against literature FDR data is added for a more detailed fuel burn investigation. The key outcomes are as follows:

- the proposed MASA is an effective tool for achieving a large improvement in the trajectory reconstruction of departing aircraft, yielding low kinematic errors with respect to the flight tracking data and reasonable estimates of thrust reduction and TOW;
- for departures of Group 1 aircraft, for which BADA4 captures the take-off thrust, BADA4 and hybrid thrust estimation methods appear to perform slightly better than ANP, with differences mostly limited to the highest climb segments (above $5,000$ *ft* AFE);
- for departures of Group 2 aircraft, for which BADA4 underestimates the take-off thrust, the ANP method seems more accurate than both BADA4 (at low height) and hybrid method (above $5,000$ *ft* AFE), showing good reliability regardless of the aircraft model;
- the fuel burn predictions obtained using the open-data solution based on ICAO Doc 9889 and AEED are about 40 % lower than those relying on the BADA4 method;
- the comparison between Doc 9889 predictions and fuel burn amounts from literature FDR data on two Boeing aircraft models yields a lower underestimation, about 20 %.

These outcomes show that methods based on easily accessible ANP data appropriately combined with open information can provide a reasonably accurate estimation of the aircraft performance during departure operations. Nevertheless, improvements should be carried out on multiple levels. Concerning the MASA, higher reliance on ADS-B seems possible for identifying additional performance-related elements, such as the engine thrust cutback instant. Moreover, further validation of thrust and fuel burn predictions may come from new FDR or QAR datasets, but their confidentiality is likely to limit the data availability to just a few aircraft configurations. Finally, indirect validations pointing to new development paths will come from results on airport noise and pollutant emission estimations based on the present modelling approach.

Funding statement

The authors are grateful to the European Commission for supporting this work, performed within the NEEDED project, funded by the European Climate, Infrastructure and Environment Executive Agency (Grant Agreement no. 101095754). This publication solely reflects the authors' view and neither the EU, nor the Funding Agency can be held responsible for the information it contains.

CRediT authorship contribution statement

Lorenzo Dorbolò: Writing – review & editing, Writing – original draft, Visualization, Validation, Software, Methodology, Investigation, Formal analysis, Data curation. **Marco Pretto:** Writing – review & editing, Writing – original draft, Validation, Supervision, Software, Resources, Methodology, Investigation, Conceptualization. **Pietro Giannattasio:** Writing – review & editing, Supervision, Software, Resources, Project administration, Funding acquisition, Conceptualization.

Declaration of competing interest

The authors declare that they have no known competing financial interests or personal relationships that could have appeared to influence the work reported in this paper.

Acknowledgements

This document has been created with or contains elements of Base of Aircraft Data (BADA) Family 4 Release 4.2 which has been made available by EUROCONTROL to UNIVERSITÀ DEGLI STUDI DI UDINE. EUROCONTROL has all relevant rights to BADA. ©2021 The European Organisation for the Safety of Air Navigation (EUROCONTROL). All rights reserved. EUROCONTROL shall not be liable for any direct, indirect, incidental, or consequential damages arising out of or in connection with this product or document, including with respect to the use of BADA.

Data availability

Datasets related to BADA4 are proprietary information and cannot be shared. All other datasets are freely available and have been referenced accordingly.

References

[1] IATA, ``Global air passenger demand reaches record high in 2024," [Online]. Available: https://www.iata.org/en/pressroom/2025-releases/2025-01-30-01/. [Accessed 2 August 2025].

[2] T. Krauth, J. Morio, X. Olive, B. Figuet, Advanced collision risk estimation in terminal manoeuvring areas using a disentangled variational autoencoder for uncertainty quantification, Eng. Appl. Artif. Intell. 133 (2024) 108137, https://doi.org/10.1016/j.engappai.2024.108137.

[3] J. Sun, L. Basora, X. Olive, M. Strohmeier, M. Schafer, OpenSky report 2022: evaluating aviation emissions using crowdsourced open flight data, in: IEEE/AIAA 41st digital avionics systems conference (DASC), Portsmouth, VA, USA, 2022, https://doi.org/10.1109/DASC55683.2022.9925852.

[4] ASCENT - Aviation Sustainability Center, Project 045 Takeoff/Climb analysis to support AEDT aircraft performance model (APM) development, ASCENT, 2020.

[5] A. Nuic, D. Poles, V. Mouillet, BADA: an advanced aircraft performance model for present and future ATM systems, Int. J. Adapt. Control Signal. Process. 24 (2010) 850–866, https://doi.org/10.1002/acs.1176.

[6] Subsonic.aero Ltd, "FLIGHT-X, multi-disciplinary aircraft flight software," [Online]. Available: https://www.subsonic.aero/flight-x. [Accessed 17 July 2025].

[7] A. Filippone, M. Zhang, N. Bojdo, Validation of an integrated simulation model for aircraft noise and engine emissions, Aerosp. Sci. Technol. 89 (2019) 370–381, https://doi.org/10.1016/j.ast.2019.04.008.

[8] M. Zhang, A. Filippone, Optimum problems in environmental emissions of aircraft arrivals, Aerosp. Sci. Tech. 123 (2022) 107502, https://doi.org/10.1016/j.ast.2022.107502.

[9] Lissys Ltd, "Piano," [Online]. Available: https://www.lissys.uk/. [Accessed 15 April 2025].

[10] D. Poll, U. Schumann, A simple model for the estimation of turbofan engine performance in all airborne phases of flight, Aeronaut. J. 128 (2024) 2725–2753, https://doi.org/10.1017/aer.2024.92.

[11] B. Graver, D. Rutherford, S. Zheng, CO2 emissions from commercial aviation - 2013, 2018 and 2019, International council on clean transportation, Washington DC, USA, 2020.

[12] Regulation (EU) 2023/1770, in: Official journal of the European union, 228, European Commission, 2023, pp. 39–48.

[13] M. Schäfer, M. Strohmeier, V. Lenders, I. Martinovic, M. Wilhelm, Bringing up OpenSky: a large-scale ADS-B sensor network for research, in: IPSN'14: proceedings of the 13th international symposium on information processing in sensor networks, Berlin, Germany, 2014, https://doi.org/10.1109/IPSN.2014.6846743.

[14] J. Sun, J.M. Hoekstra, J. Ellerbroek, OpenAP: an open-source aircraft performance model for air transportation studies and simulations, Aerospace 7 (8) (2020) 104, https://doi.org/10.3390/aerospace7080104.

[15] J. Sun, I. Dedoussi, Evaluation of aviation emissions and environmental costs in Europe using OpenSky and OpenAP, Eng. Proc. 13 (1) (2021) 5, https://doi.org/10.3390/engproc2021013005.

[16] J. Wang, H. Zhang, J. Yu, F. Lu, Y. Li, Modeling civil aviation emissions with actual flight trajectories and enhanced aircraft performance model, Atmosphere (Basel) 15 (10) (2024) 1251, https://doi.org/10.3390/atmos15101251.

[17] L. Basora, A. Chevrot, Uncertainty assessment of fuel consumption based on open data, J. Open Aviat. Sci. 1 (2) (2023), https://doi.org/10.59490/joas.2023.7233.

[18] A. Filippone, B. Parkes, N. Bojdo, T. Kelly, Prediction of aircraft engine emissions using ADS-B flight data, Aeronaut. J. 125 (1288) (2021) 988–1012, https://doi.org/10.1017/aer.2021.2.

[19] ECAC, Doc 29 4th edition: report on standard method of computing noise contours around civil airports - volume 1: applications guide, ECAC Neuilly-sur-Seine France, 2016.
[20] ECAC, Doc 29 4th edition: report on standard method of computing noise contours around civil airports - volume 2: technical guide, ECAC Neuilly-sur-Seine France, 2016.
[21] M. Pretto, P. Giannattasio, M. De Gennaro, A. Zanon, H. Kühnelt, Web data for computing real-world noise from civil aviation, Transp. Res. D: Transp. Environ. 69 (2019) 224–249, https://doi.org/10.1016/j.trd.2019.01.022.
[22] M. Pretto, P. Giannattasio, M. De Gennaro, A. Zanon, H. Kuehnelt, Forecasts of future scenarios for airport noise based on collection and processing of web data, Eur. Transp. Res. Rev. 12 (1) (2020) 1–14, https://doi.org/10.1186/s12544-019-0389-x.
[23] W. Guo, W. Zeng, Y. Zhou, A copula-ECAC model for estimating aviation noise around airports, Transp. Res. D: Transp. Environ. 142 (2025) 104666, https://doi.org/10.1016/j.trd.2025.104666.
[24] G.S. Roque, J. Reichmuth, Automating the estimation of noise and emissions near airports with ADS-B data, J. Open Aviat. Sci. 2 (2) (2024), https://doi.org/10.59490/joas.2024.7901.
[25] EASA - ANP, "Aircraft noise and performance (ANP) data," [Online]. Available: https://www.easa.europa.eu/en/domains/environment/policy-support-and-research/aircraft-noise-and-performance-anp-data. [Accessed 11 May 2025].
[26] M. Pretto, P. Giannattasio, M. De Gennaro, Mixed analysis-synthesis approach for estimating airport noise from civil air traffic, Transp. Res. D: Transp. Environ. 106 (2022) 103248, https://doi.org/10.1016/j.trd.2022.103248.
[27] M. Pretto, L. Dorbolò, P. Giannattasio, A. Zanon, Aircraft operation reconstruction and airport noise prediction from high-resolution flight tracking data. Transportation research part D: transport and environment, Transp. Res. D: Transp. Environ. 135 (2024) 104397, https://doi.org/10.1016/j.trd.2024.104397.
[28] R.C. van der Grift, M. Snellen, A. Amiri-Simkooei, The effect of using N1% as input for aircraft noise modelling, Transp. Res. D: Transp. Environ. 142 (2025) 104710, https://doi.org/10.1016/j.trd.2025.104710.
[29] G. Jarry, R. Dalmau, P. Very, J. Sun, On the generalization properties of deep learning for aircraft fuel flow estimation models, Transp. Res. C Emerg. Technol. 176 (2025) 105143, https://doi.org/10.1016/j.trc.2025.105143.
[30] ICAO, Doc 9889 - airport air quality manual - second edition, ICAO, Montréal, Canada, 2020.
[31] D. DuBois, G.C. Paynter, "Fuel flow method2" for estimating aircraft emissions, SAE Trans. 115 (2006) 1–14. https://www.jstor.org/stable/44657657.
[32] EASA, "ICAO aircraft engine emissions databank (AEED)," [Online]. Available: https://www.easa.europa.eu/en/domains/environment/icao-aircraft-engine-emissions-databank. [Accessed 23 April 2025].
[33] X. Olive, Traffic, a toolbox for processing and analysing air traffic data, J. Open. Source Softw. 4 (39) (2019) 1518, https://doi.org/10.21105/joss.01518, 1-3.
[34] D. Megginson, "OurAirports," [Online]. Available: https://ourairports.com/. [Accessed 27 April 2025].
[35] The OpenStreetMap Foundation, "OpenStreetMap," [Online]. Available: https://www.openstreetmap.org/. [Accessed 24 June 2025].
[36] S.C. Verbrugge, "Airlinerlist.com," [Online]. Available: https://plane-list.net/. [Accessed 17 April 2025].
[37] R. Zeman, "Rzjets," [Online]. Available: https://rzjets.net/aircraft/. [Accessed 28 July 2025].
[38] EASA, "ANP aircraft substitutions," [Online]. Available: https://www.easa.europa.eu/en/domains/environment/policy-support-and-research/aircraft-noise-and-performance-anp-data/anp-aircraft-substitutions. [Accessed 15 September 2025].
[39] J. Sun, H.A. Blom, J. Ellerbroek, J.M. Hoekstra, Particle filter for aircraft mass estimation and uncertainty modeling, Transp. Res. C Emerg. Technol. 205 (2019) 145–162, https://doi.org/10.1016/j.trc.2019.05.030.
[40] K.M. Mullen, Continuous global optimization in R, J. Stat. Softw. 60 (2014) 1–45, https://doi.org/10.18637/jss.v060.i06.
[41] D. Kraft, A software package for sequential quadratic programming. Deutsche forschungs- und versuchsanstalt für luft- und raumfahrt, 1988.
[42] U.S. DOT Volpe Center, Aviation environmental design tool (AEDT) version 3g - technical manual. Federal aviation administration, U.S. Department of Transportation, Washington DC, USA, 2024.
[43] EUROCONTROL Experimental Centre, User manual for the base of aircraft data (BADA) family 4, EUROCONTROL, 2016.
[44] D.A. Senzig, G.G. Fleming, R.A. Iovinelli, Modeling of terminal-area airplane fuel consumption, J. Aircr. 46 (4) (2009) 1089–1093, https://doi.org/10.2514/1.42025.